sustainability

MDPI

Article

Taking Advantage of Invasive *Eupatorium adenophorum* Plant for Eco-Synthesis and Stabilization of Nanosilver towards Durably Coloristic and Bioactive Silk Materials

Qing Li [1,2,†], Kang Gao [1,†], Yan Liang [1], Run Lu [1], Jiahe Hang [1], Huiyu Jiang [1,3,*] and Yuyang Zhou [2,*]

[1] Hubei Key Laboratory of Biomass Fibers and Eco-Dyeing & Finishing, College of Chemistry and Chemical Engineering, Wuhan Textile University, Wuhan 430200, China
[2] Jiangsu Engineering Research Center of Textile Dyeing and Printing for Energy Conservation, Discharge Reduction and Cleaner Production, China National Textile and Apparel Council Key Laboratory of Natural Dyes, College of Textile and Clothing Engineering, Soochow University, Suzhou 215006, China
[3] National Innovation Center of Advanced Dyeing and Finishing Technology, Tai'an 271000, China
* Correspondence: huiyujiang@wtu.edu.cn (H.J.); yuyangzhou@suda.edu.cn (Y.Z.); Tel.: +86-18896500651 (Y.Z.)
† These authors contributed equally to this work.

Abstract: Recently, a growing emphasis has been placed on taking advantage of invasive plants for fabricating value-added and functional materials. In the present study, an easy and efficient approach to developing durably coloristic, antioxidant and antimicrobial silk using silver nanoparticles (AgNPs) prepared with the extract of an invasive weed—*Eupatorium adenophorum* (EA)—which plays dual roles of bio-based reductant and stabilizer. The impact of factors including pH, concentration of EA extract (EAE) and Ag^+ ions, temperature and time during AgNPs synthesis against the nanoparticle size and distribution, and the AgNPs concentration, were explored. The relationship between the color feature of silk and the treatment conditions was investigated through a central composite experimental analysis. Finally, the antioxidant and antimicrobial activities as well as the washing durability of the AgNPs-decorated silk were demonstrated. The results revealed that the size of AgNPs also decreases when pH ranges from 7.7 to 10.1. The zeta potential of AgNPs is −18.3 mV due to the existence of EAE on the surface of AgNPs. AgNPs generated efficiently within first 30 min, and then slowed down from 30 to 60 min. Based on the mathematical modeling study, a theoretical highest KS of 6.95 is able to be obtained using the processing condition of AgNPs/EAE conc. 2.32 g/L; pH 2.65, temperature 68.6 and time 42.6 min. The silk decorated with AgNPs/EAE killed over 95% of *E. coli* and *S. aureus* within 24 h. The superb antimicrobial activity of the AgNPs-treated silk is contributed by the AgNPs that enable the microbial cell membrane damage and segmentation. After 30 times repeated washing, the antimicrobial activity of the treated silk still remained over 85% against both strains. In all, the functionalization of silk established in this work not only reduces the ecological destructions and economic losses induced by EAE, but also permits the obtaining of sustainably developed value-added, safe and functional textiles.

Keywords: biosynthesis; silver nanoparticle; natural extract; silk; antimicrobial; durability

Citation: Li, Q.; Gao, K.; Liang, Y.; Lu, R.; Hang, J.; Jiang, H.; Zhou, Y. Taking Advantage of Invasive *Eupatorium adenophorum* Plant for Eco-Synthesis and Stabilization of Nanosilver towards Durably Coloristic and Bioactive Silk Materials. *Sustainability* **2022**, *14*, 16668. https://doi.org/10.3390/su142416668

Academic Editors: Hafeezullah Memon, Xiaoke Jin, Wei Tian and Chengyan Zhu

Received: 15 November 2022
Accepted: 9 December 2022
Published: 13 December 2022

1. Introduction

Fast-adaptive, -growing, and -propagating invasive weeds such as *Eupatorium adenophorum* (EA) have been confirmed to induce ecological destructions and economic losses [1]. Utilization of invasive weeds is an emerging research field with a promising applicable future to control and manage EA, which enables economic transformation of agricultural byproducts and environmental hazards into valuable industrial materials, and further applied to generate new functional products that are finally beneficial to humans and society. EA is a frequently seen invasive weed that extensively invades the southern area of China [2]. In recent years, EA has been applied to the production of biopesticide, bio

sorbents, etc. [3,4]. Recent reports indicate that around a hundred bio-based bioactive compounds have been detected in *E. adenophorum* extract [5,6]. Effective utilization of EA turns waste towards profitable resources. Our recent study has also confirmed that flavonoids (e.g., "myricetin and patuletin") are the main constituents of EA extract (EAE) and further successfully applied it for green dyeing and finishing of wool [7].

Silk is a natural protein fiber and had a high reputation as a luxury textile material for thousands of years, thanks to its pleasant appearance and wearing comfortableness. Silk has also been recognized as an appropriate medical-use material owing to its superior overall performance [8–10]. However, silk products are facing critical challenges such as microbial attachment and propagation due to its protein nature that provides a suitable environment for microbial cells, thus leading to the generation of undesirable effects to the textile itself and the customers [11]. Great efforts are required to overcome these disadvantages to further expand the application area of silk products.

Silver nanoparticles (AgNPs) are among the most attractive and efficient microbial-killing nanomaterials, having a variety of commercialization applications [12,13]. To date, a number of physical and chemical fabricating methods have been developed to synthesize AgNPs [14,15]. The current challenge is how to reduce the hazardous chemicals (e.g., "reducing agent"), and the generation of toxic by-products. Biological synthesis of AgNPs is a widely confirmed sustainable approach, in which a great number of natural substances are taken advantage of [16–18]. Such a process has also been highlighted for its biological safety, and nearly zero environmental contamination. Another merit of applying flavonoids in AgNPs synthesis is that flavonoids play dual roles as effective reducing/capping agents, and in the efficient generation of AgNPs with well-defined size and morphology [19,20].

Figure 1 displays the mechanism of using EAE and Ag^+ ions to prepare AgNPs. In brief, Ag^+ ions are reduced into Ag^0 and further aggregated into AgNPs, meanwhile, the hydroxyl groups of flavonoids are oxidized into quinone forms [21,22], which further attach to the AgNPs surface. This research aims to prepare coloristic and bioactive silk fabric integrating AgNPs/EAE. The synthesis factors such as concentrations and pH were explored. The color features of AgNPs-finished silk as a function of the treatment condition was explored by mathematical modeling based on the central composite design (CCD) of the experiment. Finally, the antioxidant/antimicrobial activities and their durability against repeated washings of AgNPs-coated silk were evaluated.

Figure 1. (**a**) Photographs of EA, chopped and dried segments and extracted powder, (**b**) Synthesis of AgNPs and their deposition on silk fabric.

2. Materials and Methods

2.1. Materials

Silk fabric was obtained from Suzhou Jiaduoli Silk Apparel Co., Ltd., Suzhou, China. EA, collected from farmland at Yuxi, Yunnan, was dried and ground into fragments. Silver nitrate was purchased from Shanghai Institute of Fine Chemical Co., Ltd., Shanghai, China. A commercial detergent Honder SW ECO was used for the washing test. All other chemicals were analytical grade. All water used was ultrapure water.

2.2. Extraction and Purification

Extraction of EA was implemented by using 40% ethanol solution with a solid-to-liquid ratio of 1:60 at pH 7 under 80 °C. The purification process was carried out through a dynamic sorption-desorption method using DM301 macroporous adsorption resin. More details are described in our recent research [7].

2.3. AgNPs Fabrication

Five mL of $AgNO_3$ (1 mM) was added slowly at a rate of 5 mL/min into one mL of EAE (50 g/L) along with additional water towards 50 mL at pH of 9.2 regulated by sodium carbonate solution, and then oscillated at 70 °C for 30 min. To demonstrate the pH impact on the UV–vis adsorption feature and nano size, the pH value was ranged from 7.7 to 10.1 using sodium carbonate. In terms of the concentration study, 0.2~2 g/L of EAE and 0.1~1.5 mM $AgNO_3$ were used.

2.4. Incorporation of AgNPs to Silk

One gram of silk fabric was dropped into a 50 mL AgNPs suspension. The pH was regulated by acetic acid in the range of 3–6. The temperature was set constant during fabric treatment in a range of 50 to 90 °C with a processing time of 30 to 60 min. The resultant fabrics were thoroughly washed and dried and stored for further test. To explore the impact of the treatment conditions and their internal interactions on the color feature of silk as well as the optimal treatment condition, a CCD experiment design (Table 1) was formed with the aid of a trial version of Minitab software.

Table 1. Variables and factorial matrix.

Run Order	V_1: Conc. (g/L)	V_2: pH	V_3: Temp. (°C)	V_4: Time (min)	KS	
					Actual	Predicted
1	1	3	60	50	4.03	4.18
2	1	3	80	30	4.05	4.16
3	1	3	60	30	3.31	3.41
4	1.5	6	70	40	3.21	3.12
5	1.5	4	70	60	5.40	5.21
6	1.5	4	70	40	5.80	5.93
7	2	5	60	30	3.96	4.08
8	1.5	4	70	40	5.89	5.93
9	2	3	80	30	5.81	5.87
10	2	3	60	30	5.70	5.80
11	1.5	4	70	40	5.90	5.93
12	1	5	80	50	3.91	3.98
13	2.5	4	70	40	6.12	5.96
14	2	5	80	30	3.74	3.76
15	1.5	4	50	40	4.47	4.27
16	1.5	2	70	40	5.84	5.61
17	1	5	60	50	3.70	3.81
18	0.5	4	70	40	3.40	3.23
19	1.5	4	70	40	6.10	5.93
20	1.5	4	70	40	5.70	5.93
21	1	5	80	30	3.12	3.21

Table 1. *Cont.*

Run Order	V_1: Conc. (g/L)	V_2: pH	V_3: Temp. (°C)	V_4: Time (min)	KS	
					Actual	Predicted
22	1	3	80	50	4.71	4.74
23	2	3	60	50	6.29	6.36
24	1.5	4	70	20	4.02	3.88
25	1.5	4	90	40	4.64	4.51
26	2	5	80	50	4.26	4.31
27	1	5	60	30	2.85	2.85
28	1.5	4	70	40	5.90	5.93
29	2	5	60	50	4.77	4.82
30	2	3	80	50	6.07	6.24
31	1.5	4	70	40	6.20	5.93

2.5. Measurements

2.5.1. Characterizations of AgNPs

UV-vis spectra and absorbance were obtained by a Shimadzu UV-1800 UV–visible spectrophotometer. The size/distribution/zeta potential were taken from a Zetasizer Nano ZS 90 at 25 °C with 90° detection angle based on the dynamic light scattering analysis. The spherical morphology of particles was observed using an HT7700 transmission electron microscope (TEM) at an accelerating voltage of 100 kV. The average size and polydispersity were calculated by image analysis software. The XRD patterns were taken from an X'Pert-Pro MPD diffractometer using Cu-Kα radiation. Before TEM and XRD measurements, the AgNPs suspension was subject to a purification process to obtain clear TEM image and intense XRD curves, respectively.

2.5.2. Characterizations of Treated Silk

The fabrics obtained as described in Section 2.4, Incorporation of AgNPs to silk, are used for characterizations. The fabric surface was observed by Hitachi S-4800 SEM using 3.0 kV acceleration voltage. The a*/b* values representing the color features of the fabric, were measured by Datacolor 600. For the washing test, the fabrics were put in 2 g/L detergent solution with a total volume of 50 mL and subject to stirring for 15 min at 50 °C. Such procedure was repeated 10 and 30 times to get 10 and 30 washing cycles. The Ag content was measured by ICP-OES according to Equation (1):

$$\text{Ag content } (\text{mg/g}) = \frac{C_s}{W} \times V \quad (1)$$

where C_s is the Ag concentration in the digestion solution analyzed by ICP-OES; V is the volume of the digestion solution; W is the weight of dried sample.

The antimicrobial activities of fabrics were evaluated based on GB/T 20944.3-2008 according to Equation (2):

$$\text{Antimicrobial activity } (\%) = \frac{N_{ctrl} - N_{spl}}{N_{ctrl}} \times 100 \quad (2)$$

where N_{ctrl} and N_{spl} are the quantities of the visible bacterial colonies of standard fabric and tested fabric, respectively.

E. coli (ATCC 8099) and *S. aureus* (ATCC 6538) were adopted for this test. The tested fabrics (0.75 g) were cut into square pieces, dropped in the conical flasks and shaken with bacteria solution for 24 h at 24 °C. The bacteria suspension was diluted to 1k times, inoculated onto agar plates and incubated at 37 °C for 24 h.

Antioxidant activity: The antioxidant activity was evaluated using the ABTS method [19]. The ABTS radical cation ($ABTS^+$), formulated by 7 mM ABTS solution and 2.45 mM potassium persulfate, was kept in the dark at room temperature for 12 h before use. After

dilution with phosphate buffer (pH 7.4) towards an abs of 0.7 at 734 nm, 10 mg fibers was dropped into 10 mL $ABTS^+$ solution. After 30 min, the scavenging capability of $ABTS^+$ at 734 nm was calculated using Equation (3):

$$\text{Antioxidant activity } (\%) = \frac{A_{ctrl} - A_{spl}}{A_{ctrl}} \times 100 \quad (3)$$

where A_{ctrl} and A_{spl} are the initial and remaining abs of the ABTS solutions, respectively.

3. Results

3.1. AgNPs Fabrication

3.1.1. Size and Quantity Manipulation

During the generation of AgNPs in aqueous solution, it is speculated that the concentrations of Ag^+ (oxidative composition) and flavonoids (reducing composition), pH value (influencing the reducing capability of flavonoids), temperature (affecting the speed of NPs generation), and time (related to the total quantity of AgNPs) are the major factors in relationship with the size and quantity of the AgNPs in suspension. These two characteristics are highly related to the final color feature and antimicrobial activity of the silk materials. Therefore, the manipulation of the size and quantity of AgNPs against the concentrations of Ag^+/flavonoids, pH value, temperature, and time, should be understood before application.

pH: Flavonoids were confirmed as the major components in EAE in our previous study [7]. It is also known that the solubility, dissociation extent, and reducing ability of flavonoids are highly related to pH values, which further influences AgNPs generation. As depicted in Figure 2a, there are two intensive bands located in 300–400 nm and 240–280 nm wavelength ranges in the UV-Vis absorption spectrum of the EAE solution. The front band (I) indicates the presence of cinnamoyl systems (B/C rings) and the later one is the clue to the presence of benzoyl systems (A/C rings) [23]. Those are the characteristic bands of flavonoids. Interestingly, the color of EAE solution quickly turned from yellow to dark brown in half a minute when Ag^+ ion solution was added dropwise. Based on such a phenomenon, the successful fabrication of AgNPs is preliminarily confirmed. The fast color response of EAE solution indicates its high reducing ability to turn Ag^+ ions to Ag. In terms of the UV-Vis adsorption spectra, a new maximum absorption at around wavelength of 400 nm occurred in each spectrum compared with pure EAE solution. In fact, these maximum absorptions are the optical detection of AgNPs due to their surface plasmon resonance behavior [24]. Importantly, the Abs intensity at λ_{max} increases along with the pH elevating. Such a result suggests that more AgNPs are generated at higher pH value, because of the deeper deprotonation of the phenolic groups in flavonoids that contributes to the greater reducing action [25]. The size of AgNPs also decreases when pH ranges from 7.7 to 10.1 (See Figure 2a). The zeta potential of AgNPs is −18.3 mV (Figure 2b) due to the existence of EAE on the surface of AgNPs which contributes to repulsion of neighboring AgNPs from aggregation. The larger size of AgNPs indicates the heavier aggregation of AgNPs during synthesis, which may be due to the lower electrostatic repellence at lower pH values. Moreover, a blue-shifting phenomenon occurred on these new maximum absorptions when pH increased, which is related to the size decrease of AgNPs [26].

Concentration: Both concentrations of EAE and Ag^+ ions are significant to the nucleation of AgNPs. Specifically, EAE plays the dual roles of reducing and capping agent, which control the speed of Ag^+ transformation into Ag, and the stability of nanoparticles by capping out layer of particles, respectively. When the EAE concentration increases, the Abs intensity that represents the yield quantity of AgNPs increases (Figure 3a), which demonstrates that EAE facilitates the generation of AgNPs. Moreover, EAE enables the production of AgNPs smaller than 60 nm, which is not only due to the mild reducing property of EAE but also its capping behavior; in other words, both properties prevent the AgNPs from aggregation during nucleation. This is one advantage of making use of

EAE for AgNPs synthesis rather than using synthetic reducing and stabilizing agents. By further increasing the EAE concentration, the AgNPs become smaller. In fact, the actual size of AgNPs is smaller than the results obtained by DLS method. This is due to the stabilizing effect of the EAE which coated the out layer of the AgNPs; however, DLS detects the size of the whole nanocomposites [27]. In addition, PDI decreases greatly at higher concentrations of EAE, which indicates the promoted uniformity of size distribution. Conversely, increasing the Ag^+ concentration increases the size of nanoparticles but decreases the uniformity (Figure 3b). The reason for this phenomenon is similar to the analysis of the EAE concentration above, which means the relative concentrations of the EAE and Ag^+ is significant, rather than their respective concentrations.

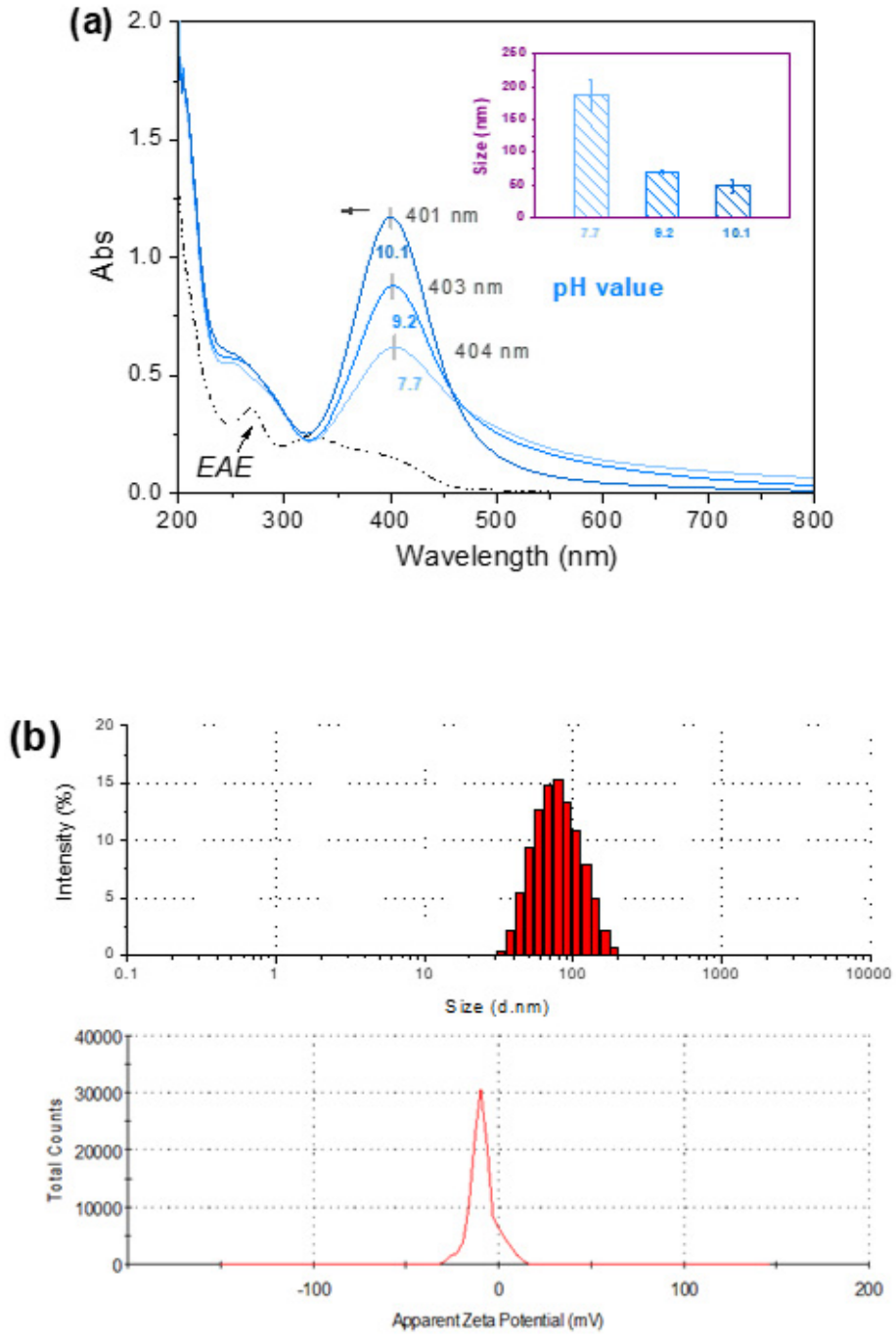

Figure 2. (**a**) UV–Vis absorption spectra of AgNPs synthesized by EAE at pH changes, (**b**) size distribution and zeta potential of AgNPs suspension.

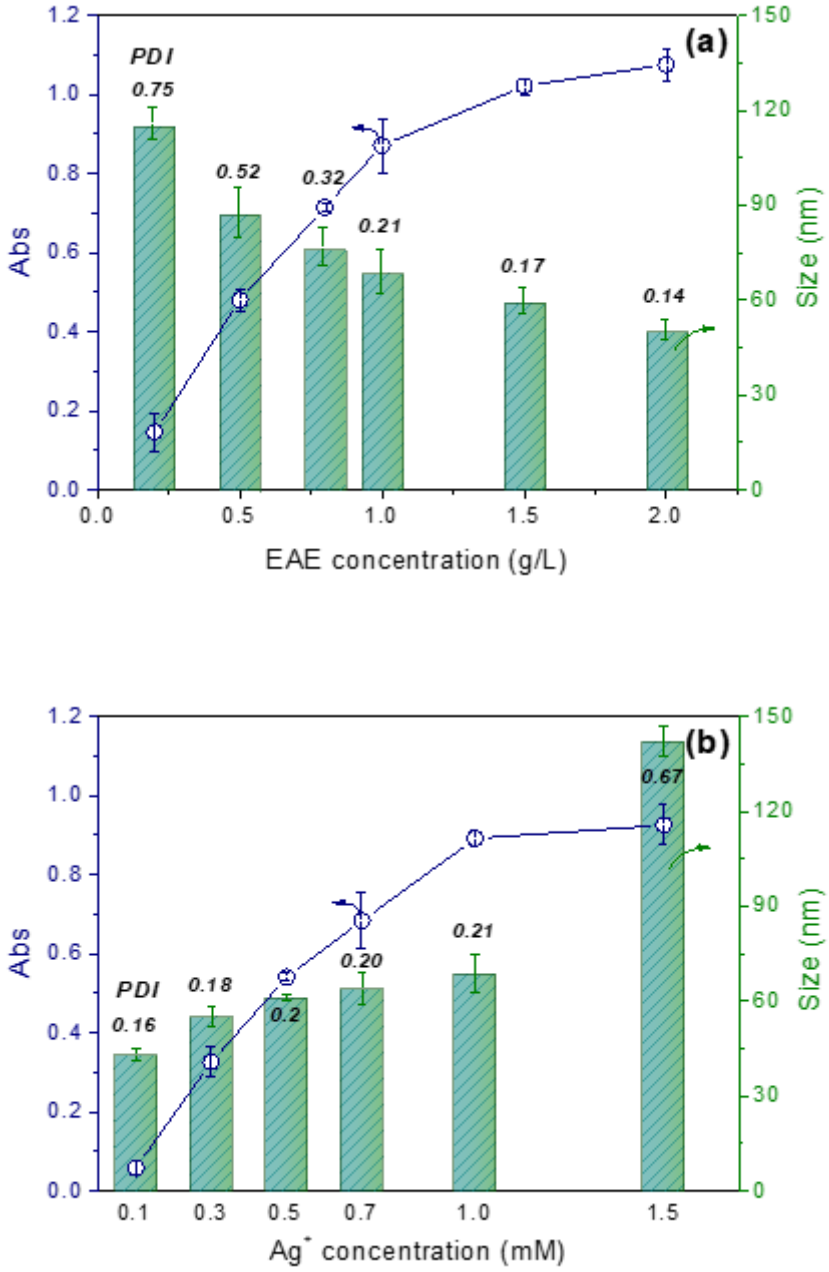

Figure 3. Absorbance, average particle size and PDI of the AgNPs synthesized by various concentrations of (**a**) EAE and (**b**) Ag^+ ions (95% significance).

Temperature and time: The temperature during AgNPs synthesis is related to the forming speed of nuclei, thus, to well control the temperature contributes to the good manipulation of quantity and particle size of AgNPs. As seen in Figure 4a, more AgNPs were fabricated at higher temperature indicated by the elevating Abs intensity. This result is in alignment with previous studies [25,28]. The size of AgNPs varies mildly from 40 to 70 nm in the temperature range of 30 to 70 °C. However, a sudden increase of particle size and PDI appears at 90 °C, resulting from the intensified agglomeration and decreased uniformity of AgNPs at high temperature. With regard to these analyses, 70 °C is a proper temperature that well controls the yield, particle size, and uniformity of AgNPs, and was applied in the following experiment. To investigate the AgNPs fabricating behavior as a function of processing time, the Abs intensity of AgNPs suspension was monitored at constant temperature. The temperature was stabilized at 30 °C considering the accuracy of measurements due to the superfast nucleation phenomenon that took place at high

temperature. Figure 4b shows that the AgNPs generated efficiently within first 30 min, and then slowed down from 30 to 60 min. This indicates the efficient reduction reaction that took place in the presence of EAE. The above experiments demonstrate the successful preparation of AgNPs using EAE. Such AgNPs synthesis process has four advantages: (1) non-toxic bio-based reductant from EAE is used; (2) EAE performs dual roles of reducing and stabilizing agents instead of using synthetic reducing and capping agents; (3) non-toxic solvent–water makes the resultant AgNPs available for the direct application to fabric treatment; (4) the rapid fabrication of AgNPs using mild processing conditions contributes to the reduction of energy consumption and promotion of synthesis efficiency. These fulfil the requirements of green chemistry and sustainable development [29].

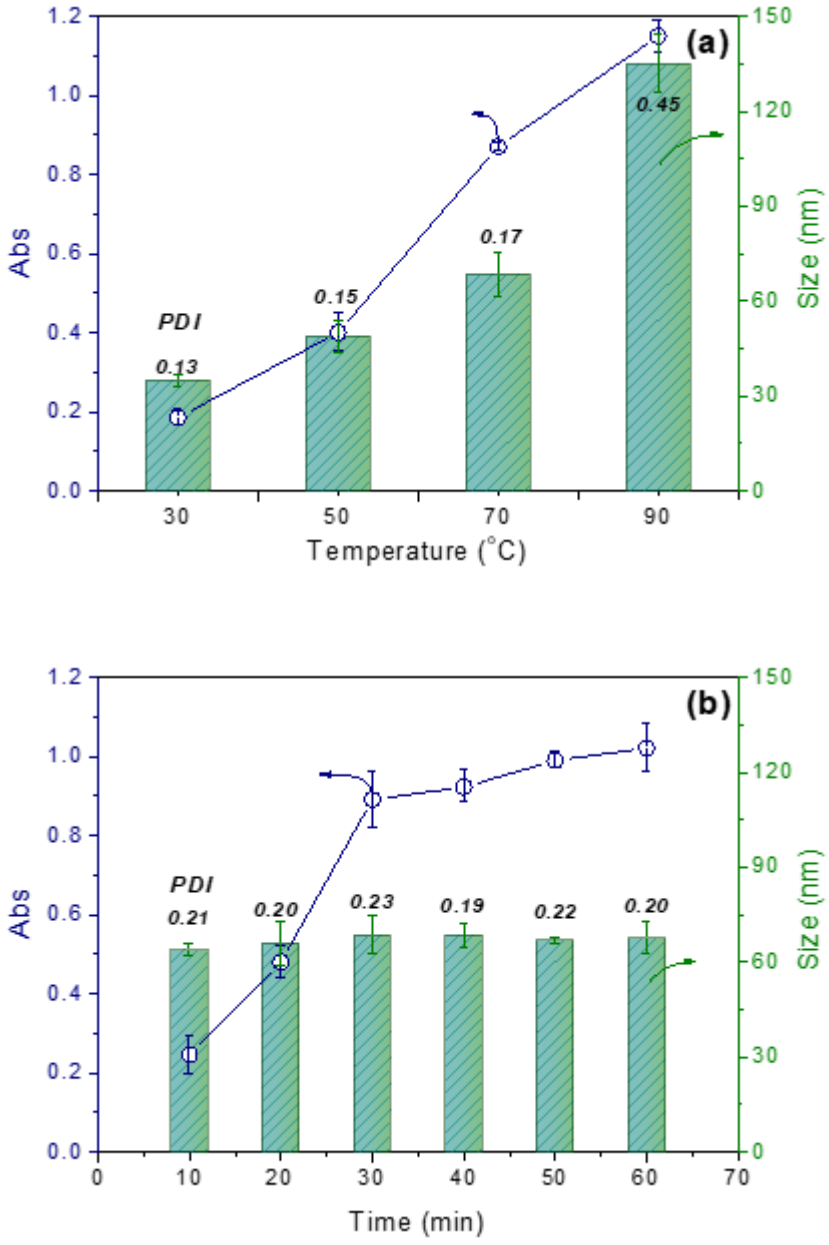

Figure 4. Abs, particle size and PDI of the AgNPs synthesized under different (**a**) temperatures and (**b**) processing time (95% significance).

3.1.2. XRD and TEM

The XRD patterns in Figure 5a show obvious peaks at 38.3°, 44°, 64.6°, and 77.4°, which correspond to the (111), (200), (220), and (311) Braggs reflections of Ag face-centered

cubic structure, respectively. Those peaks are well matched with the standard JCPDS file No. 04-0783. Such result manifests the crystalline nature of the resultant AgNPs. TEM was further used to explore the morphology and size distribution of the AgNPs prepared with EAE. As displayed in Figure 5b, most AgNPs have spherical morphology and show well monodispersing feature. The size of the AgNPs distributes in the range of 56–71 nm, and this is close to the DLS results shown in Figure 2b above.

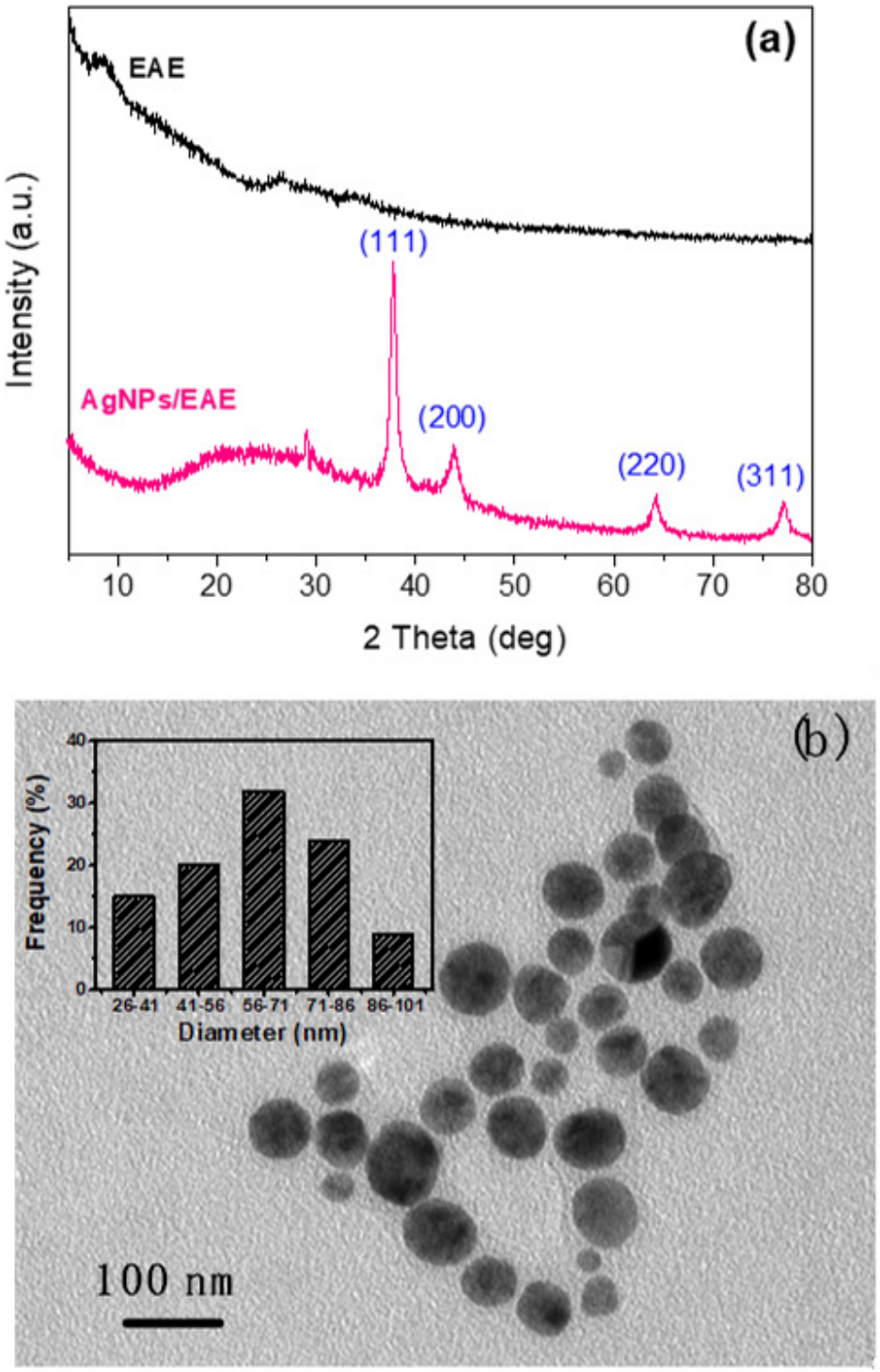

Figure 5. (**a**) XRD pattern and (**b**) TEM image for AgNPs fabricated with EAE.

3.2. Application of AgNPs

3.2.1. CCD Experiment

To systematically investigate the factors' impacts and interactions on the color depth of the AgNPs-decorated silk, and to further optimize the parameters, a CCD experiment was carried out and analysed using mathematical modelling software. Four variables were included which are AgNPs/EAE concentration (0.5~2.5 g/L), pH (3~6), temperature (50~90 °C) and time (30~60 min) denoted as V_1, V_2, V_3 and V_4. The equation describing the relationship between these variables and the KS value of fabric is formed:

$$K/S = A + B*V_1 + C*V_2 + D*V_3 + E*V_4 + F*V_1*V_2 + G*V_1*V_3 + H*V_1*V_4 + I*V_2*V_3 + J*V_2*V_4 + K*V_3*V_4 + L*V_1^2 + M*V_2^2 + N*V_3^2 + O*V_4^2$$

where V_1, V_2, V_3 and V_4 are variables; A is the constant; B~O are the coefficients of terms. By mathematical modelling, the equation is obtained as follows.

$$KS = -39.93 + 10.509*Conc. + 3.871*pH + 0.6513*Temp. + 0.3392*Time - 1.333*Conc.*Conc. - 0.3914*pH*pH - 0.003832*Temp.*Temp. - 0.003457*Time*Time - 0.5800*Conc.*pH - 0.03425*Conc.*Temp. - 0.01075*Conc.*Time - 0.00975*pH*Temp. + 0.00475*pH*Time - 0.000463*Temp.*Time$$

The corresponding data analysis exported from the software is displayed in Table 2. In general, the 'lack-of-fit' analysis shows a *p*-value of 0.414 which is obviously higher than 0.05 (threshold level), which indicates the good fitness of the established model to describe the relationships between variables (V_1~V_4) and response (KS). Further, the high R-sq. (98.56%) quantitively reconfirms the fitness of the model. The close percentage of adjusted R-sq. (97.31%) and predicted R-sq. (93.80%) demonstrates the appropriateness of using such a model to predict the experimental results. The P-values of most coefficients are smaller than 0.001, indicating their significance in the KS value of fabricated silk, except the *p*-values for the linear coefficient of Temp. and two-way interactive coefficients including Conc.*Time, pH*Time and Temp.*Time. This indicates that manipulating the temperature during the AgNPs loading to silk could not make an obvious change to the color depth of the treated silk. In fact, the color depth is highly dependent on the loading quantity of AgNPs on silk. As the AgNPs are around 80 nm in size, which is much larger than ordinary dyes or finishers in molecular state, the expansion of silk at high temperature could marginally induce the 'adsorption' of AgNPs to the fiber inertia. In terms of the interactions, Conc.*Time, pH*Time and Temp.*Time, hardly any interactive behaviors were detected. For the interactions between Conc. and pH, the reason may be due to the fact that the pH relates to the dissociation status of capped flavonoids over the AgNPs, further influencing the extent of AgNPs aggregations in the suspension, which therefore corresponds to the total concentration of AgNPs. The significance of these terms are in alignment with the Pareto Chart displayed in Figure 6a, and the main effects in Figure 6b. A set of 2D contour plots were obtained from the software and displayed in Figure 6c, which perceptively describes the interactions between each two variables. The dark violet zone indicates the high KS value. It is obvious that to decrease pH and increase the concentration enables the KS enhancement. This is because a lower pH induces higher numbers of cationized amino groups on silk for more negatively charged (EAE adsorbed on the surface) AgNPs to stabilize. However, the median temperature (around 70 °C) and processing time (around 45 min) facilitates better color yield. To be specific, the AgNPs display reduced stability at high temperature towards aggregation in the suspension before being captured by silk. Longer processing time not only induces the decline of the AgNPs stability, but also increase the propensity of AgNPs to detach from silk fibers. Thus, a calculated optimal condition is generated based on the established model. The theoretical highest KS of 6.95 is able to be obtained using the processing condition of AgNPs/EAE conc. 2.32 g/L; pH 2.65, temperature 68.6 and time 42.6 min.

Table 2. Analysis of Variance and Model Summary.

Analysis of Variance					
Source	**DF**	**Adj SS**	**Adj MS**	**F-Value**	***p*-Value**
Model	14	36.7732	2.6267	78.50	<0.001
Linear	4	23.1652	5.7913	173.07	<0.001
Conc.	1	11.1521	11.1521	333.28	<0.001
pH	1	9.2866	9.2866	277.53	<0.001
Temp.	1	0.0864	0.0864	2.58	0.128
Time	1	2.6401	2.6401	78.90	<0.001
Square	4	11.5246	2.8811	86.10	<0.001
Conc.*Conc.	1	3.1744	3.1744	94.87	<0.001
pH*pH	1	4.3798	4.3798	130.89	<0.001
Temp.*Temp.	1	4.1987	4.1987	125.48	<0.001
Time*Time	1	3.4171	3.4171	102.12	<0.001
2-Way Interaction	6	2.0835	0.3472	10.38	<0.001
Conc.*pH	1	1.3456	1.3456	40.21	<0.001
Conc.*Temp.	1	0.4692	0.4692	14.02	0.002
Conc.*Time	1	0.0462	0.0462	1.38	0.257
pH*Temp.	1	0.1521	0.1521	4.55	0.049
pH*Time	1	0.0361	0.0361	1.08	0.314
Temp.*Time	1	0.0342	0.0342	1.02	0.327
Error	16	0.5354	0.0335		
Lack-of-Fit	10	0.3605	0.0361	1.24	0.414
Pure Error	6	0.1748	0.0291		
Total	30	37.3086			
Model Summary					
S	**R-sq**	**R-sq(adj)**	**R-sq(pred)**		
0.182925	98.56%	97.31%	93.80%		

Figure 7 displays the color feature of the AgNPs-modified silk fabrics using a*/b* values as the indictors which are shown in the color coordinate according to the CIE color system. Untreated silk has very small a*/b* values approaching to the origin point in the color coordinate, which demonstrates its colorless nature. The silk fabrics modified with AgNPs are dark brownish in color. Moreover, the a*/b* values of treated silk continually reduced towards the origin point of the coordinate at higher concentration of AgNPs used. This result implies the reduced color saturation which is visibly seen as a dull color. Similar observation has also been recorded in a previous study [30], in which the progressive change in color appearance was related to augmenting the amount of Ag deposited on the silk surface. These results demonstrate that AgNPs/EAE is able to impart silk with a coffee color, besides other functions such as antimicrobial activity.

3.2.2. Surface Morphology

The untreated/treated silk was subjected to surface morphological imaging, which is shown in Figure 8. The sample was fabricated using 1 g/L EAE and 1 mM $AgNO_3$. Obviously, the untreated silk is smooth and clean. With respect of AgNPs-treated silk, large quantities of spherical-shaped AgNPs are detected in a uniform distribution on the fiber surface, some of which are monodispersed (See examples in blue circles) and others are combined particles (See examples in red circles). It is interesting to find that some of AgNPs on the fiber surface are larger than 100 nm in diameter, which is larger than the results obtained by DLS and TEM analyses. One reason for this phenomenon is the aggregation of AgNPs induced by high surface energy of AgNPs when they approached the silk surface during treatment [31]. In all, these SEM images provide evidence of the successful loading of AgNPs onto the silk surface. On the other hand, the high density and uniform dispersity of AgNPs on silk accounts for its bioactive functions.

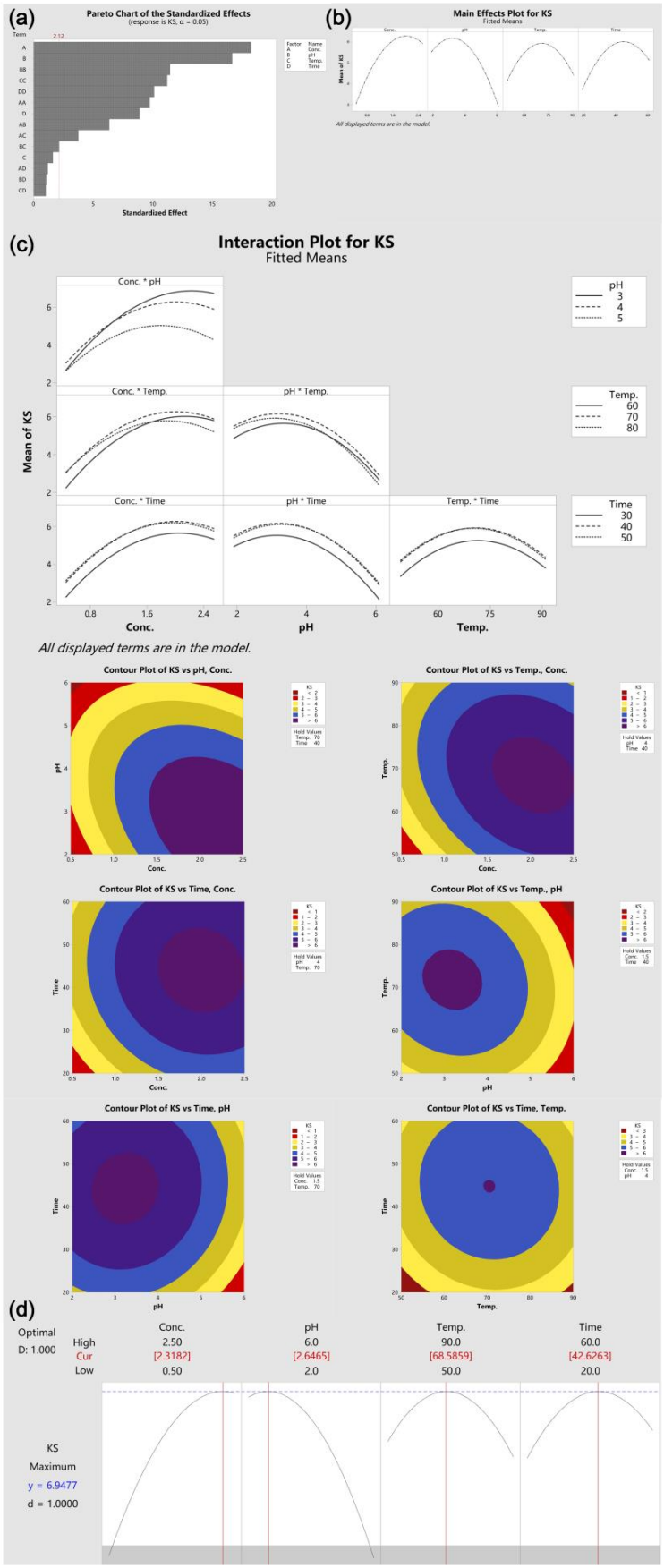

Figure 6. (**a**) Pareto chart, (**b**) Main effects, (**c**) Interaction and contour plots, and (**d**) Optimization.

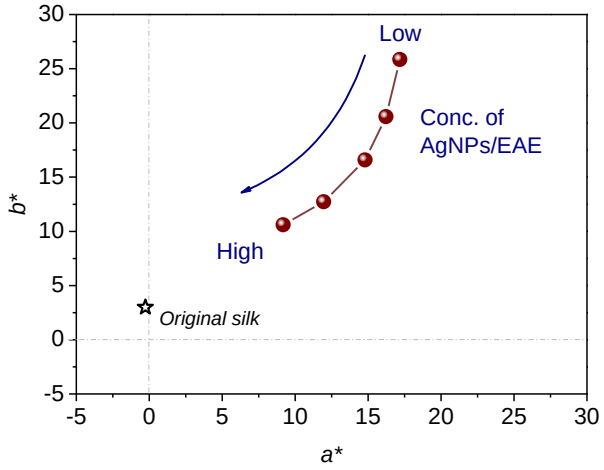

Figure 7. Color feature variation of the treated silk as a function of AgNPs/EAE concentration.

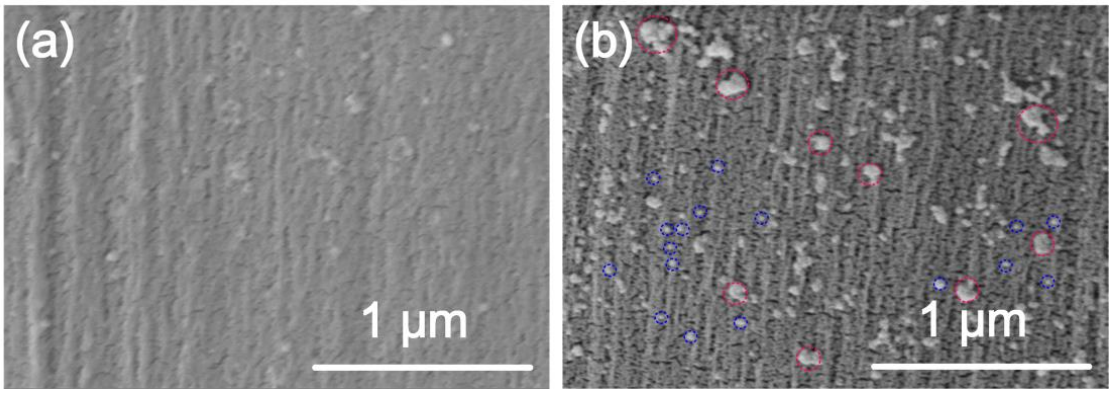

Figure 8. SEM image: (**a**) original and (**b**) AgNPs/EAE-treated silk.

3.2.3. Bioactivities and Their Washing Durability

The antimicrobial activity of the AgNPs-decorated silk was explored using *E. coli* and *S. aureus* as testing strains, which represent Gram– and Gram+, respectively. The fabric treated by 1 g/L EAE and 1 mM $AgNO_3$ was used for measurement. Untreated silk has nearly no antimicrobial function. After 24 hours' contact, the microbial reduction rate was merely 18% and 16% against *E. coli* and *S. aureus*, respectively Figure 9a. Significantly, the silk decorated with AgNPs/EAE killed over 95% of *E. coli* and *S. aureus* within 24 h. The superb antimicrobial activity of the AgNPs-treated silk id contributed by the AgNPs that enable the microbial cell membrane damage and segmentation [32]. Such behavior has also been confirmed in Figure 10. To be specific, the morphology of the *E. coli* and *S. aureus* cells was changed to segments demonstrating their perished state. The gradual release of Ag^+ ions from AgNPs is another reason for the excellent antimicrobial activity [33]. The higher microbial reduction of *E. coli* than *S. aureus* lies in the thicker cell wall of Gram+ than Gram- microbials [34,35]. A certain amount of EAE adsorbed by silk and on the AgNPs surface during the treatment imparts silk with antioxidant activity besides the antimicrobial function. After 30 repeated washes, the treated silk still showed an antimicrobial reduction rate over 85%. These findings are in alignment with the previous studies [19,20], in which baicalin, quercetin and rutin were applied for AgNPs bio-synthesis and served for the durable antibacterial finishing of silk. Previous studies have confirmed the quantity- or size-dependent toxicity of AgNPs, which includes gastrointestinal toxicity, genotoxicity and carcinogenicity, immune system toxicity, kidney toxicity, liver toxicity, etc. [6,36]. However, in our case, there is much less toxicity of AgNPs compared with those taken as medicinal treatment. With respect to the skin toxicity, researchers also concluded that the toxicity of AgNPs in human epidermal keratinocytes can be influenced by the residual contaminants

in the solutions, and that the particles themselves may not have been responsible for increased cell death [36]. Thus, further in-depth and comprehensive study on the toxicity of AgNPs-coated textile is required in the future. In general, integrating of the results of Ag content, the released AgNPs from silk fiber is also effective in killing microbials.

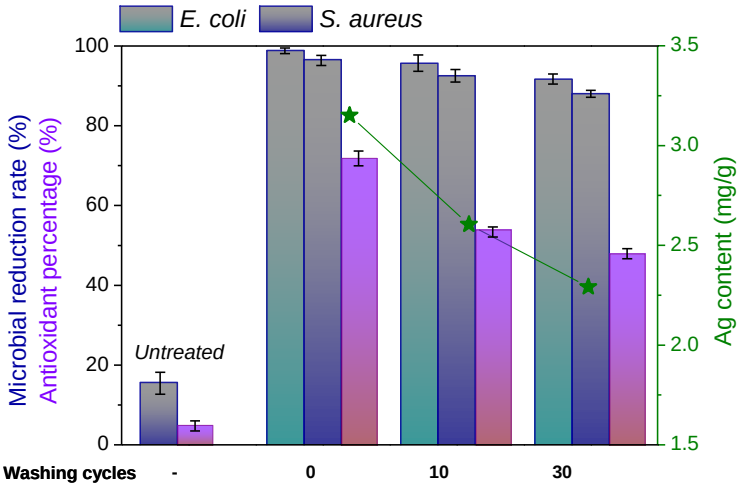

Figure 9. Antimicrobial and antioxidant activities of the AgNPs-modified silk fabric, and the corresponding durability against repeated washing (95% significance).

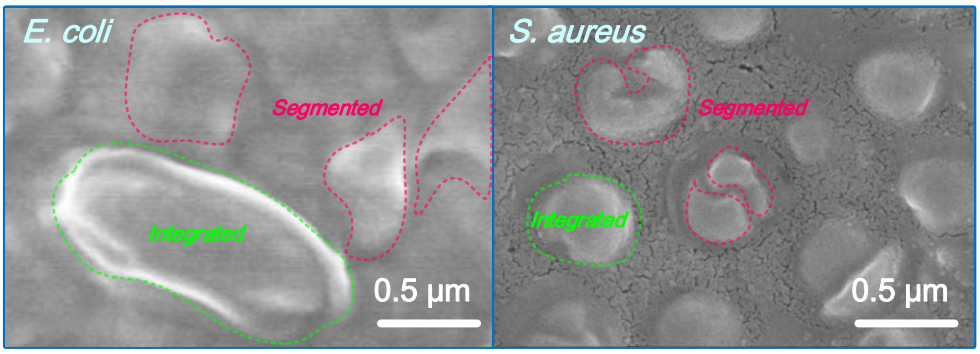

Figure 10. Morphological changes of microbial cells after interaction with AgNPs/EAE.

4. Conclusions

This study proposes an easy and sustainable approach to producing coloristic and bioactive silk textiles using AgNPs bio-synthesized by EAE. The prepared AgNPs are spherical in morphology and uniformly dispersed in the suspension, with the help of EAE as bio-based reducing/stabilizing agent. The size of AgNPs is able to be manipulated by controlling EAE and Ag^+ ion concentrations. A high quantity and uniform loading of AgNPs imparted silk fabrics with a dark brown color, excellent antimicrobial activity and a certain antioxidant activity. AgNPs-treated silk fabric retains over 85% microbial inhibition rate even after 30 wash cycles. In general, this study manifests that the AgNPs-treated silk fabrics prepared by the established method are available for medical and protective applications.

Author Contributions: Q.L.: Conceptualization, investigation, writing original draft. K.G.: data curation, formal analysis, experiment. Y.L.: data curation, formal analysis. R.L. and J.H.: data curation, experiment. H.J.: supervision, review and editing. Y.Z.: supervision, writing original draft, review and editing. All authors have read and agreed to the published version of the manuscript.

Funding: This work was supported by the Opening Project of Jiangsu Engineering Research Center of Textile Dyeing and Printing for Energy Conservation, Discharge Reduction and Cleaner Production (SDGC2101), Opening Project of China National Textile and Apparel Council Key Laboratory of Natural Dyes, Soochow University (SDHY2217), Scientific Research Fund Project of National Innovation Center of Advanced Dyeing and Finishing Technology (ZJ2021A05).

Institutional Review Board Statement: Not applicable.

Informed Consent Statement: Not applicable.

Data Availability Statement: Not applicable.

Conflicts of Interest: The authors declare no conflict of interest.

References

1. Zhang, Y.; Zhou, Q.; Rather, L.J.; Li, Q. Agricultural waste of Eriobotrya japonica L. (Loquat) seeds and flora leaves as source of natural dye and bio-mordant for coloration and bio-functional finishing of wool textile. *Ind. Crops Prod.* **2021**, *169*, 113633. [CrossRef]
2. Fan, L.; Miao, J.; Yang, J.; Zhao, X.; Shi, W.; Xie, M.; Wang, X.; Chen, W.; An, X.; Luo, H.; et al. Invasive plant-crofton weed as adsorbent for effective removal of copper from aqueous solution. *Environ. Technol. Innov.* **2022**, *26*, 102280. [CrossRef]
3. Feng, Q.; Wang, B.; Chen, M.; Wu, P.; Lee, X.; Xing, Y. Invasive plants as potential sustainable feedstocks for biochar production and multiple applications: A review. *Resour. Conserv. Recycl.* **2021**, *164*, 105204. [CrossRef]
4. Sun, X.; Lu, Z.; Sang, W. Review on studies of Eupatorium adenophoruman important invasive species in China. *J. For. Res.* **2004**, *15*, 319–322.
5. Khan, H.; Marya, A.; Amin, S.; Kamal, M.A.; Patel, S. Flavonoids as acetylcholinesterase inhibitors: Current therapeutic standing and future prospects. *Biomed. Pharmacother.* **2018**, *101*, 860–870. [CrossRef] [PubMed]
6. Giri, S.; Sahu, R.; Paul, P.; Nandi, G.; Dua, T.K. An updated review on Eupatorium adenophorum Spreng. [Ageratina adenophora (Spreng.)]: Traditional uses, phytochemistry, pharmacological activities and toxicity. *Pharmacol. Res. -Mod. Chin. Med.* **2022**, *2*, 100068. [CrossRef]
7. Li, Q.; Mei, H.; Zhang, Z.; Jiang, H.; Zhang, W. Valorization of flavonoid-rich invasive weed-Eupatorium adenophorum in the cleaner production of coloristic and functional wool fabric with a research focus on photofading mechanism. *Ind. Crops Prod.* **2022**, *189*, 115835. [CrossRef]
8. Koh, L.D.; Cheng, Y.; Teng, C.P.; Khin, Y.W.; Loh, X.J.; Tee, S.Y.; Low, M.; Ye, E.; Yu, H.D.; Zhang, Y.W.; et al. Structures, mechanical properties and applications of silk fibroin materials. *Prog. Polym. Sci.* **2015**, *46*, 86–110. [CrossRef]
9. Mottaghitalab, F.; Hosseinkhani, H.; Shokrgozar, M.A.; Mao, C.; Yang, M.; Farokhi, M. Silk as a potential candidate for bone tissue engineering. *J. Control. Release* **2015**, *215*, 112–128. [CrossRef]
10. Li, G.; Liu, H.; Li, T.; Wang, J. Surface modification and functionalization of silk fibroin fibers/fabric toward high performance applications. *Mater. Sci. Eng. C* **2012**, *32*, 627–636. [CrossRef]
11. Shahid, M.; Zhou, Y.; Tang, R.; Chen, G.; Wani, W.A. Colorful and antioxidant silk with chlorogenic acid: Process development and optimization by central composite design. *Dyes Pigm.* **2017**, *138*, 30–38. [CrossRef]
12. Rajan, R.; Chandran, K.; Harper, S.L.; Yun, S.I.; Kalaichelvan, P.T. Plant extract synthesized silver nanoparticles: An ongoing source of novel biocompatible materials. *Ind. Crops Prod.* **2015**, *70*, 356–373. [CrossRef]
13. Tolaymat, T.M.; Badawy, A.M.E.; Genaidy, A.; Scheckel, K.G.; Luxton, T.P.; Suidan, M. An evidence-based environmental perspective of manufactured silver nanoparticle in syntheses and applications: A systematic review and critical appraisal of peer-reviewed scientific papers. *Sci. Total Environ.* **2010**, *408*, 999–1006. [CrossRef]
14. Shahid-ul-Islam; Butola, B.S.; Mohammad, F. Silver nanomaterials as future colorants and potential antimicrobial agents for natural and synthetic textile materials. *RSC Adv.* **2016**, *6*, 44232–44247.
15. Thakkar, K.N.; Mhatre, S.S.; Parikh, R.Y. Biological synthesis of metallic nanoparticles. *Nanomed. Nanotechnol.* **2010**, *6*, 257–262. [CrossRef] [PubMed]
16. Mittal, A.K.; Chisti, Y.; Banerjee, U.C. Synthesis of metallic nanoparticles using plant extracts. *Biotechnol. Adv.* **2013**, *31*, 346–356. [CrossRef] [PubMed]
17. Kharissova, O.V.; Dias, H.V.R.; Kharisov, B.I.; Pérez, B.O.; Pérez, V.M.J. The greener synthesis of nanoparticles. *Trends Biotechnol.* **2013**, *31*, 240–248. [CrossRef] [PubMed]
18. Maddinedi, S.; Mandal, B.K.; Maddili, S.K. Biofabrication of size controllable silver nanoparticles—A green approach. *J. Photochem. Photobiol. B* **2017**, *167*, 236–241. [CrossRef]
19. Zhou, Y.; Yang, Z.; Tang, R. Green and facile fabrication of AgNPs@silk for colorful and multifunctional textiles using baicalin as a natural reductant. *J. Clean. Prod.* **2018**, *170*, 940–949. [CrossRef]
20. Zhou, Y.; Tang, R. Facile and Eco-Friendly Fabrication of Colored and Bioactive Silk Materials Using Silver Nanoparticles Synthesized by Two Flavonoids. *Polymers* **2018**, *10*, 404–418. [CrossRef]
21. Bulut, E.; Özacar, M. Rapid, Facile Synthesis of Silver Nanostructure Using Hydrolyzable Tannin. *Ind. Eng. Chem. Res.* **2009**, *48*, 5686–5690. [CrossRef]

22. Boroumand, M.N.; Montazer, M.; Simon, F.; Liesiene, J.; Šaponjic, Z.; Dutschk, V. Novel method for synthesis of silver nanoparticles and their application on wool. *Appl. Surf. Sci.* **2015**, *346*, 477–483. [CrossRef]
23. Anouar, E.H.; Gierschner, J.; Duroux, J.-L.; Trouillas, P. UV/Visible spectra of natural polyphenols: A time-dependent density functional theory study. *Food Chem.* **2012**, *131*, 79–89. [CrossRef]
24. Aziz, S.B.; Abdulwahid, R.T.; Rasheed, M.A.; Abdullah, O.G.; Ahmed, H.M. Polymer Blending as a Novel Approach for Tuning the SPR Peaks of Silver Nanoparticles. *Polymers.* **2017**, *9*, 486–497. [CrossRef]
25. Yang, N.; Li, W. Mango peel extract mediated novel route for synthesis of silver nanoparticles and antibacterial application of silver nanoparticles loaded onto non-woven fabrics. *Ind. Crops Prod.* **2013**, *48*, 81–88. [CrossRef]
26. Anandalakshmi, K.; Venugobal, J.; Ramasamy, V. Characterization of silver nanoparticles by green synthesis method usingPedalium murex leaf extract and their antibacterial activity. *Appl. Nanosci.* **2016**, *6*, 399–408. [CrossRef]
27. Hayakawa, K.; Yoshimura, T.; Esumi, K. Preparation of gold-dendrimer nanocomposites by laser irradiation and their catalytic reduction of 4-nitrophenol. *Langmuir* **2003**, *19*, 5517–5521. [CrossRef]
28. Rao, B.; Tang, R. Green synthesis of silver nanoparticles with antibacterial activities using aqueous Eriobotrya japonica leaf extract. *Adv. Nat. Sci. Nanosci. Nanotechnol.* **2017**, *8*, 15014–15021. [CrossRef]
29. Banach, M.; Pulit-Prociak, J. Proecological method for the preparation of metal nanoparticles. *J. Cleaner Prod.* **2017**, *141*, 1030–1039. [CrossRef]
30. Shahid, M.; Zhou, Y.; Cheng, X.; Zar, M.S.; Chen, G.; Tang, R.-C. Ferulic acid promoted in-situ generation of AgNPs@silk as functional colorants. *J. Clean. Prod.* **2018**, *176*, 736–744. [CrossRef]
31. Zhang, D.; Toh, G.W.; Lin, H.; Chen, Y. In situ synthesis of silver nanoparticles on silk fabric with PNP for antibacterial finishing. *J. Mater. Sci.* **2012**, *47*, 5721–5728. [CrossRef]
32. Tran, H.V.; Tran, L.D.; Ba, C.T.; Vu, H.D.; Nguyen, T.N.; Pham, D.G.; Nguyen, P.X. Synthesis, characterization, antibacterial and antiproliferative activities of monodisperse chitosan-based silver nanoparticles. *Colloids Surf. A* **2010**, *360*, 32–40. [CrossRef]
33. Emam, H.E.; Manian, A.P.; Široká, B.; Duelli, H.; Redl, B.; Pipal, A.; Bechtold, T. Treatments to impart antimicrobial activity to clothing and household cellulosic-textiles—Why "Nano"-silver? *J. Clean. Prod.* **2013**, *39*, 17–23. [CrossRef]
34. Kaviya, S.; Santhanalakshmi, J.; Viswanathan, B.; Muthumary, J.; Srinivasan, K. Biosynthesis of silver nanoparticles using citrus sinensis peel extract and its antibacterial activity. *Spectrochim. Acta Part A* **2011**, *79*, 594–598. [CrossRef] [PubMed]
35. Zhou, Y.; Tang, R. Facile and eco-friendly fabrication of AgNPs coated silk for antibacterial and antioxidant textiles using honeysuckle extract. *J. Photochem. Photobiol. B* **2018**, *178*, 463–471. [CrossRef]
36. Mitra, K.; Elham, G.; Shahla, K.; Zahra, H.; Afshin, M.-B. Effects of silver nanoparticles on human health. *Eur. J. Nanomed.* **2015**, *7*, 51–62.